AMERICAN SOCIETY FOR MICROBIOLOGY | mBio®

RESEARCH ARTICLE
Host-Microbe Biology

Molecular Basis for the Evolution of Species-Specific Hemoglobin Capture by *Staphylococcus aureus*

Jacob E. Choby,[a,b,c] Hanna B. Buechi,[d] Allison J. Farrand,[a] Eric P. Skaar,[a,b] Matthew F. Barber[d]

[a]Department of Pathology, Microbiology, and Immunology, Vanderbilt University Medical Center, Nashville, Tennessee, USA
[b]Vanderbilt Institute for Infection, Immunology, and Inflammation, Vanderbilt University Medical Center, Nashville, Tennessee, USA
[c]Graduate Program in Microbiology and Immunology, Vanderbilt University, Nashville, Tennessee, USA
[d]Institute of Ecology and Evolution, University of Oregon, Eugene, Oregon, USA

ABSTRACT Metals are a limiting resource for pathogenic bacteria and must be scavenged from host proteins. Hemoglobin provides the most abundant source of iron in the human body and is required by several pathogens to cause invasive disease. However, the consequences of hemoglobin evolution for bacterial nutrient acquisition remain unclear. Here we show that the α- and β-globin genes exhibit strikingly parallel signatures of adaptive evolution across simian primates. Rapidly evolving sites in hemoglobin correspond to binding interfaces of IsdB, a bacterial hemoglobin receptor harbored by pathogenic *Staphylococcus aureus*. Using an evolution-guided experimental approach, we demonstrate that the divergence between primates and staphylococcal isolates governs hemoglobin recognition and bacterial growth. The reintroduction of putative adaptive mutations in α- or β-globin proteins was sufficient to impair *S. aureus* binding, providing a mechanism for the evolution of disease resistance. These findings suggest that bacterial hemoprotein capture has driven repeated evolutionary conflicts with hemoglobin during primate descent.

IMPORTANCE During infection, bacteria must steal metals, including iron, from the host tissue. Therefore, pathogenic bacteria have evolved metal acquisition systems to overcome the elaborate processes mammals use to withhold metal from pathogens. *Staphylococcus aureus* uses IsdB, a hemoglobin receptor, to thieve iron-containing heme from hemoglobin within human blood. We find evidence that primate hemoglobin has undergone rapid evolution at protein surfaces contacted by IsdB. Additionally, variation in the hemoglobin sequences among primates, or variation in IsdB of related staphylococci, reduces bacterial hemoglobin capture. Together, these data suggest that *S. aureus* has evolved to recognize human hemoglobin in the face of rapid evolution at the IsdB binding interface, consistent with repeated evolutionary conflicts in the battle for iron during host-pathogen interactions.

KEYWORDS *Staphylococcus aureus*, evolution, heme transport, hemoglobin, host-pathogen interactions, iron acquisition

Animals possess a variety of molecular factors that effectively sequester essential metals from invasive microbes, contributing to an innate immune function termed nutritional immunity (1, 2). Iron, as a critical cofactor for many host and bacterial enzymes, has provided the paradigm for our current understanding of nutritional immunity. Since the discovery of iron limitation by egg white ovotransferrin in the 1940s (3), the mechanisms underlying nutritional immunity and bacterial iron scaveng-

Received 13 July 2018 **Accepted** 10 October 2018 **Published** 20 November 2018

Citation Choby JE, Buechi HB, Farrand AJ, Skaar EP, Barber MF. 2018. Molecular basis for the evolution of species-specific hemoglobin capture by *Staphylococcus aureus*. mBio 9:e01524-18. https://doi.org/10.1128/mBio.01524-18.

Editor Kimberly A. Kline, Nanyang Technological University

Address correspondence to Eric P. Skaar, eric.skaar@vanderbilt.edu, or Matthew F. Barber, mfbarber@uoregon.edu.

ing have been the subject of intense study (4). Many vertebrate-associated bacteria harbor high-affinity uptake systems targeting heme, an abundant iron-containing porphyrin cofactor (5).

The most abundant source of heme iron in the mammalian host is hemoglobin, which mediates oxygen transport within circulating erythrocytes. The predominant adult hemoglobin consists of a tetramer containing two α-globin and two β-globin protein subunits, each of which binds a single heme molecule for the coordination of oxygen. The Gram-positive bacterium *Staphylococcus aureus* is well adapted to the human host and is a leading cause of skin and soft tissue infections, endocarditis, osteomyelitis, and bacteremia (6). To acquire iron during infection, *S. aureus* has evolved a high-affinity hemoglobin binding and heme extraction system, termed the iron regulated surface determinant (Isd) system (7). Following the lysis of proximal erythrocytes via secreted bacterial toxins, the released hemoglobin is captured by receptors at the *S. aureus* cell surface (8, 9). The Isd system of *S. aureus* in part consists of cell wall-anchored IsdB and IsdH, which bind hemoglobin and haptoglobin-hemoglobin, respectively (9, 10).

We and others have shown that IsdB is the primary hemoglobin receptor for *S. aureus* and critical for pathogenesis in murine infection models (9, 11–13). Additionally, IsdB is highly expressed in human blood (14) and a promising vaccine target (15), underscoring its importance in human disease. IsdB extracts heme from hemoglobin, and heme is subsequently passed across the cell wall and into the cytoplasm for degradation by the heme oxygenases IsdG and IsdI, liberating iron (16–20). Underscoring the importance of IsdB for pathogenesis, heme is the preferred iron source of *S. aureus* during murine infection (21). The cell wall-anchored IsdABCH proteins share between one and three NEAT (near transporter) domains for the coordination of hemoglobin or heme. IsdB NEAT1 binds hemoglobin while NEAT2 binds heme, tethered by an intervening linker (22). Consistent with the adaptation of *S. aureus* to colonize and infect humans, we previously found that *S. aureus* IsdB binds human hemoglobin more effectively than mouse hemoglobin, the common laboratory animal used to model *S. aureus* infection (13). These results suggest that hemoglobin variation among mammals dictates effective heme acquisition by *S. aureus* and other Gram-positive bacteria.

Previous work has demonstrated that pathogens can promote a rapid adaptation of host immunity genes through repeated bouts of positive selection (23–25). While adaptation during such evolutionary conflicts can take many forms, theoretical and empirical studies indicate that an elevated rate of nonsynonymous to synonymous substitutions in protein-coding genes is often indicative of recurrent positive selection (26, 27). To date, most empirical studies of host-pathogen "arms races" have focused on viruses (28–31). Recently, we showed that the transferrin family of iron-binding proteins has undergone extremely rapid evolution in primates at protein surfaces bound by iron acquisition receptors from Gram-negative bacteria (32, 33). These findings are consistent with the existence of a long-standing evolutionary conflict for nutrient iron, whereby mutations in iron-binding proteins that prevent bacterial scavenging protect the host from infection and are favored by natural selection. While these studies have expanded our understanding of how pathogens shape the evolution of host genomes, they also raise the question of whether other components of nutritional immunity might be subject to similar evolutionary dynamics.

In addition to its role as the principal bloodstream oxygen transporter, hemoglobin has provided an important biological model for diverse areas of the life sciences. Elegant studies have illustrated how hemoglobin variation underlies multiple instances of adaptation to high altitudes in diverse vertebrate taxa (34–37). Hemoglobin alleles have also likely been subject to the balance of selection in human populations, where mutations that produce sickle-cell disease also confer resistance to severe malaria (38) and have reached high frequencies in regions where malaria is endemic. Despite its long history of study, the consequences of hemoglobin evolution for vertebrate nutritional immunity remain unclear. In the present study, we set out to investigate the

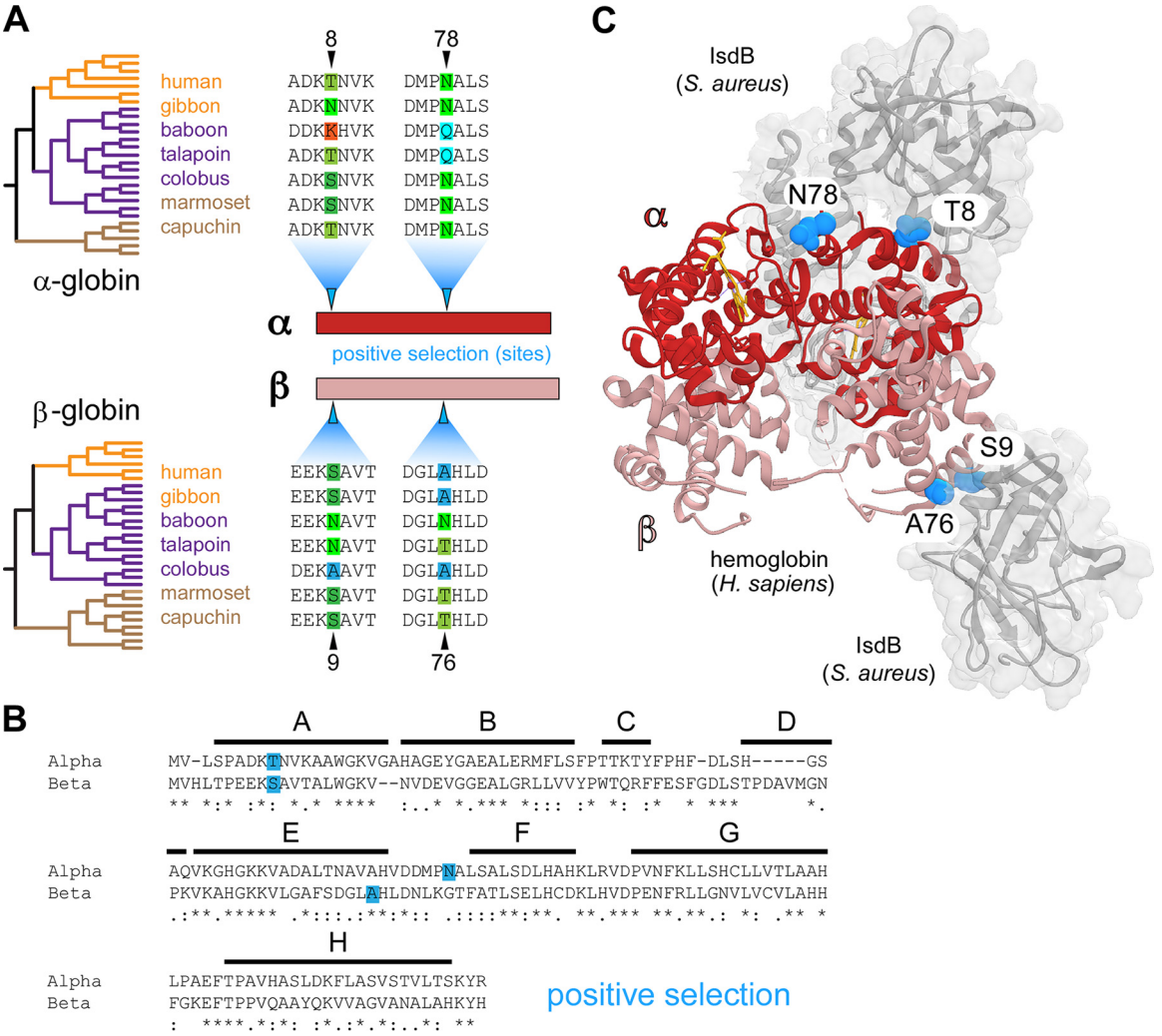

FIG 1 Parallel signatures of positive selection among primate hemoglobins at the bacterial IsdB binding interface. (A) Species phylogenies for the 27 α-globin and 30 β-globin orthologs analyzed (left). Alignments from representative species across hominoid (orange), Old World monkey (purple), and New World monkeys (brown) are shown, the full phylogenetic trees are displayed in Fig. 3 and 4. Amino acid sites under positive selection were identified in α-globin and β-globin (blue arrows) using PAML with both species and gene trees (posterior probabilities, $>$0.95). (B) Amino acid alignment of human α-globin and β-globin proteins. The position of conserved helices A to H are shown, and identity between globins is noted as conserved (*), highly similar (:), and similar (.). (C) The residues of α-globin (red) and β-globin (salmon) under positive selection (blue spheres) at the interface of hemoglobin capture by *Staphylococcus aureus* IsdB (gray) (PDB 5VMM).

evolution of hemoglobin family proteins in primates and determine whether primate hemoglobin evolution impacts the ability to sequester heme iron from bacterial pathogens.

RESULTS

Parallel signatures of positive selection in primate hemoglobins at the IsdB binding interface. To investigate how natural selection has shaped hemoglobin diversity in simian primates, orthologs of the α- and β-globin genes were cloned and sequenced from primate cell lines as well as compiled from publicly available databases. In total, 27 α-globin and 30 β-globin orthologs were assembled for phylogenetic analyses using the PAML and HyPhy software packages (Fig. 1A; see also Materials and Methods), which use nonsynonymous and synonymous substitution rates to infer signatures of positive selection. Because globin genes have been shown to undergo gene conversion, which can distort inferred phylogenetic relationships (39, 40), all analyses were performed using both a well-supported species tree as well as gene trees

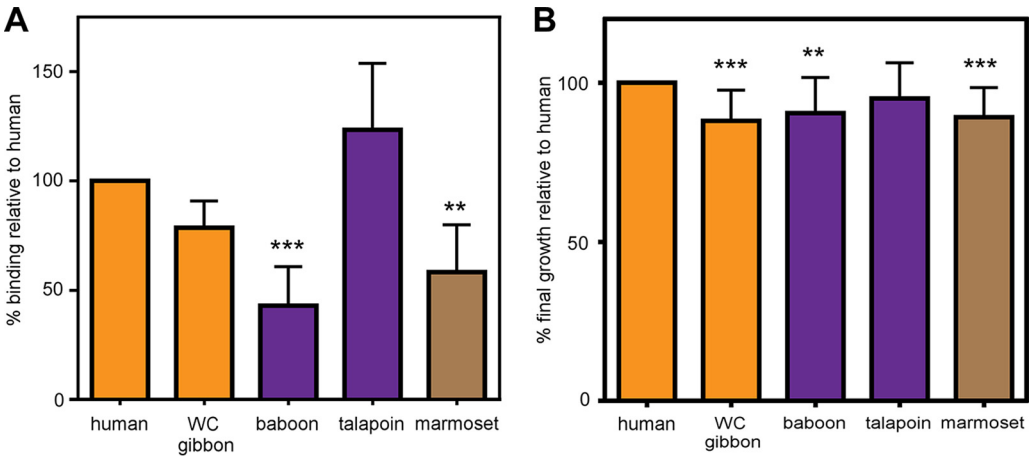

FIG 2 Primate hemoglobin variation dictates *S. aureus* binding and heme iron acquisition. (A) *S. aureus* binding of recombinant hemoglobin of various primate species. An iron-starved *S. aureus* wild type was incubated with purified recombinant hemoglobin from representative species across hominoid (orange), Old World monkey (purple), and New World monkeys (brown). Hemoglobin bound to the surface of *S. aureus* was eluted and analyzed by SDS-PAGE; relative hemoglobin abundance was measured by densitometry analysis (Image J) and compared to human hemoglobin for each replicate. (B) Growth of *S. aureus* in iron-depleted medium with 2.5 μg/ml of purified recombinant hemoglobin as the sole iron source. Shown is the final growth yield of *S. aureus* after 48 h. Growth of each replicate is compared to growth using human hemoglobin. Panel A shows the means from two independent experiments in biological triplicates, panel B shows the means from three independent experiments with 2 to 3 biological replicates, $\pm$ SEM; **, $P < 0.005$; ***, $P < 0.0005$ by two-way analyses of variance (ANOVA) with Sidak's correction for multiple comparisons comparing transformed (percent value) data.

generated using PhyML. All tests detected significant evidence of positive selection acting on both α- and β-globins using both species and gene phylogenies (see Data Set S1 in the supplemental material). Multiple analyses repeatedly identified two sites in α- and β-globins exhibiting strong signatures of positive selection (Fig. 1A). It became apparent that these rapidly evolving sites localized to similar regions of the α- and β-globin proteins, specifically, the N-terminal A helix and the hinge region between the E and F helices (Fig. 1B). In fact, the two sites exhibiting signatures of selection in the α- and β-globin A helices are at homologous positions. These parallel signatures of selection between α- and β-globins might indicate that a similar selective pressure has driven this divergence between primate species. To investigate whether bacterial heme-scavenging receptors are one such selective pressure, rapidly evolving sites were mapped onto a recently solved cocrystal structure between human hemoglobin and the IsdB protein from *S. aureus* (22). Notably, all four rapidly diverging hemoglobin residues are localized to the IsdB binding interface, in close proximity to the NEAT1 domain (Fig. 1C). Altogether, these findings indicate that primate globins have undergone rapid divergence at specific sites proximal to the binding interface of the *S. aureus* hemoglobin receptor IsdB.

Primate hemoglobin variation dictates *S. aureus* binding and heme iron acquisition. To assess how hemoglobin divergence among primates impacts recognition by *S. aureus*, recombinant hemoglobin from human, white-cheeked gibbon, baboon, talapoin, and marmoset sources were purified, providing a broad representation from our phylogenetic data set. An established biochemical assay was used to measure the binding of hemoglobin by *S. aureus*, in which *S. aureus* cells recognize recombinant human hemoglobin as well as hemoglobin purified from blood in an IsdB-dependent manner (see Fig. S1). *S. aureus* exhibited significantly reduced binding of baboon and marmoset hemoglobin to the cell surface (Fig. 2A and S2). It was noted that the binding patterns did not strictly match the predictions based on host phylogeny, suggesting discrete large-effect substitutions in hemoglobin may contribute disproportionately to the recognition by *S. aureus*. We next determined the ability of primate hemoglobins to support growth of *S. aureus* as the sole iron source. Consistent with the whole-cell binding data, hemoglobins that were bound by *S. aureus* with low affinity were unable

to support optimal bacterial growth, indicating that the capability to bind hemoglobin is a measure of the ability to utilize hemoglobin as an iron source (Fig. 2B and S3). Altogether, these results demonstrate that variation among primate globins dictates bacterial hemoglobin capture and heme-dependent growth.

Species-specific diversity in α-globin restricts heme scavenging by *S. aureus*. The identification of rapidly evolving sites at the IsdB binding interface in both α-globin and β-globin suggests that both globin subunits contribute to *S. aureus* species-specific hemoglobin capture. We therefore exploited the enhanced binding of human hemoglobin relative to that from baboon to examine the role of each globin subunit in this biochemical interaction. The ability of *S. aureus* to bind chimeric hemoglobins was measured, which revealed that both globins contribute to species specificity (Fig. 3A and S4A), as chimeras containing either human α- or β-globin were bound more effectively than baboon hemoglobin. However, α-globin appears to have a greater effect on human-specific capture, as the α-human β-baboon chimera bound significantly better than α-baboon β-human. Focusing on phylogenetic variation at the protein binding interface, α-globin T8 and N78 were found to both be proximal to the NEAT1 domain of IsdB (Fig. 3B and C). Mutagenesis of the N-terminal alpha helix of human α-globin revealed that substituting the Thr residue of human α-globin with the Lys residue of baboon α-globin at position 8 reduced binding by *S. aureus* (Fig. 3D and S4B and C). Additionally, replacing A5D, T8K, and N9H in human α-globin, which converts this seven-amino-acid region (Fig. 3B), with those of baboon α-globin leaves *S. aureus* binding nearly indistinguishable from that of baboon hemoglobin. These results demonstrate that the N-terminal helix of α-globin makes a major contribution to human-specific hemoglobin recognition by *S. aureus*. Next, the relative importance of the rapidly evolving N78 residue in α-globin was assessed, which lies N terminal to the sixth alpha helix (Fig. 3B). The substitution of N78 for a glutamine (present in baboon, talapoin, and other Old World primates) or a histidine reduced the binding of human hemoglobin (Fig. 3E and S4D). Thus, substitutions at multiple residues in α-globin that exhibit signatures of repeated positive selection are sufficient to disrupt the ability of *S. aureus* to recognize human hemoglobin.

β-Globin divergence contributes to *S. aureus* hemoglobin binding. *S. aureus* was capable of binding the baboon α-globin human β-globin chimeric hemoglobin with higher affinity than baboon hemoglobin (Fig. 3A), signifying that β-globin also contributes to *S. aureus* species-specific hemoglobin capture. Therefore, the contribution of rapidly evolving residues in β-globin to this binding interaction was investigated (Fig. 4A). Both S9 and A76 interact closely with the NEAT1 domain of IsdB (Fig. 4B). The effect of replacing the human β-globin S9 and A76 with residues found in other primate species analyzed in this work was systematically tested, which revealed that A76 is particularly important for binding by *S. aureus* (Fig. 4C and S5). Notably, baboon and human β-globins differ at both positions 9 and 76, suggesting that these residues contribute to the inability of IsdB to bind baboon hemoglobin. These differences might also explain the different binding affinities between human hemoglobin and the human α-globin baboon β-globin chimera, observed in Fig. 3A. As for α-globin, no single residue substitution improved binding by *S. aureus* IsdB, consistent with the hypothesis that IsdB has specifically adapted to bind human hemoglobin. Taken together with earlier data, residues at the IsdB interface of both α-globin and β-globin contribute to the recognition of hemoglobin by *S. aureus*. This is consistent with the NEAT1 domain of multiple IsdB monomers engaging in hemoglobin capture by binding both α- and β-globins, as observed in the reported cocrystal structure (22).

IsdB diversity among related staphylococcal strains impacts primate-specific hemoglobin capture. Given the observed differences in *S. aureus* binding between diverse primate hemoglobins, we considered how genetic variation in IsdB might impact this interaction. The IsdB NEAT1 subdomain Q162R-S170T is critical for hemoglobin recognition and is completely conserved among more than three thousand *S. aureus* clinical isolates (11). Therefore, IsdB variation among congeneric *Staphylococcus argenteus* and *Staphylococcus schweitzeri* was assessed. These recently diverged taxa

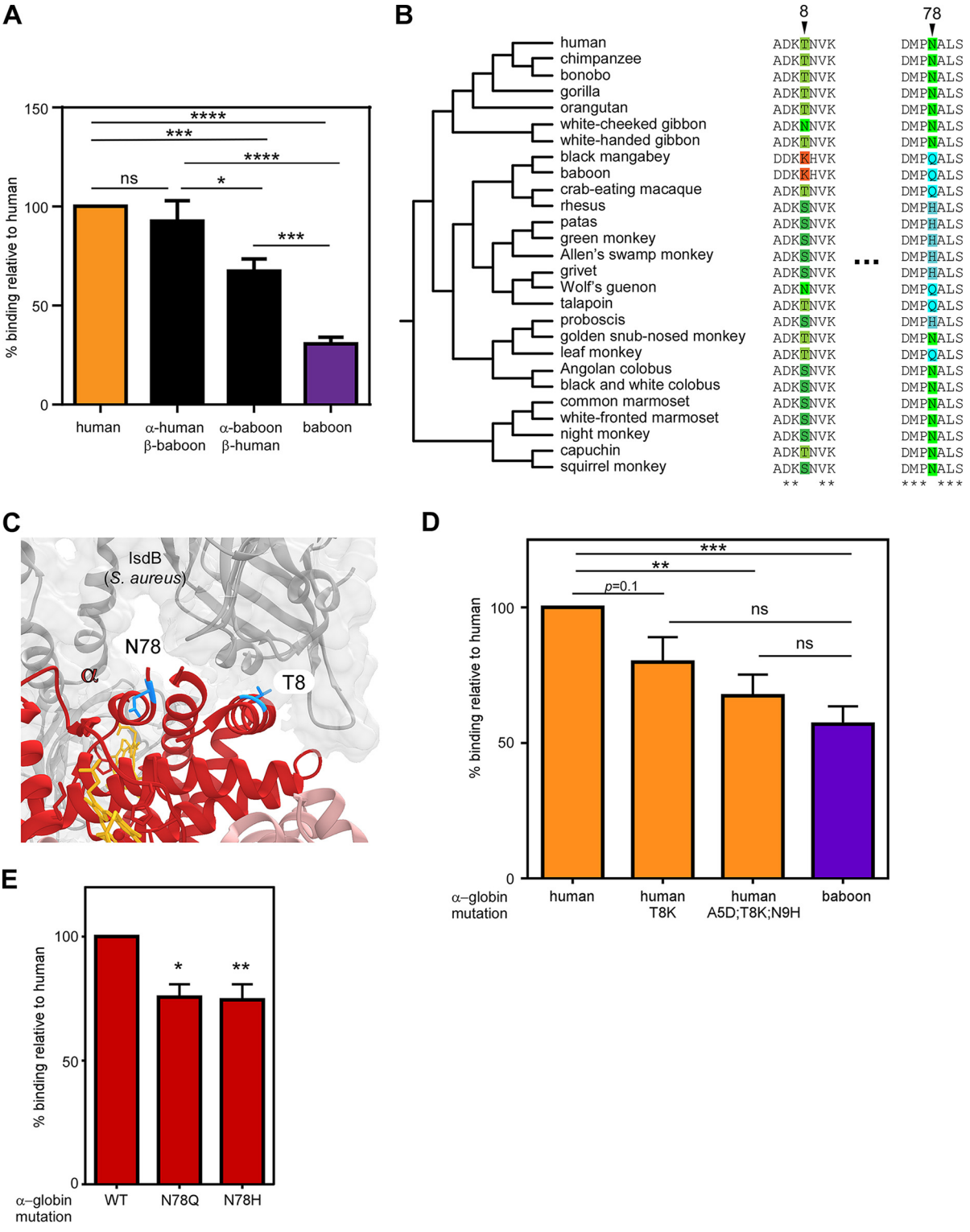

FIG 3 Species-specific diversity in α-globin restricts heme scavenging by *S. aureus*. (A). An iron-starved *S. aureus* wild type was incubated with purified recombinant hemoglobin, and bound hemoglobin was quantified. (B) Species phylogenies and sequence alignments surrounding positions exhibiting signatures of positive selection in α-globin. (C) Residues 8 and 78 of human α-globin (red) interact closely with IsdB (gray) (PDB 5VMM). (D) An iron-starved *S. aureus* wild type was incubated with purified recombinant hemoglobin, including mutagenized human hemoglobin, and bound hemoglobin was quantified. (E) An iron-starved *S. aureus* wild type was incubated with purified recombinant hemoglobin, including mutagenized human hemoglobin, and bound hemoglobin was quantified. Panel A shows the means from 3 independent experiments with 2 to 3 biological replicates, panel D shows the means from 6 independent experiments with 2 to 3 biological replicates, and panel E shows the means from 2 independent experiments with 3 biological replicates ± SEM; ns, no significance; *, $P < 0.05$; **, $P < 0.005$; ***, $P < 0.0005$ by two-way ANOVA with Sidak's correction for multiple comparisons comparing transformed (percent value) data.

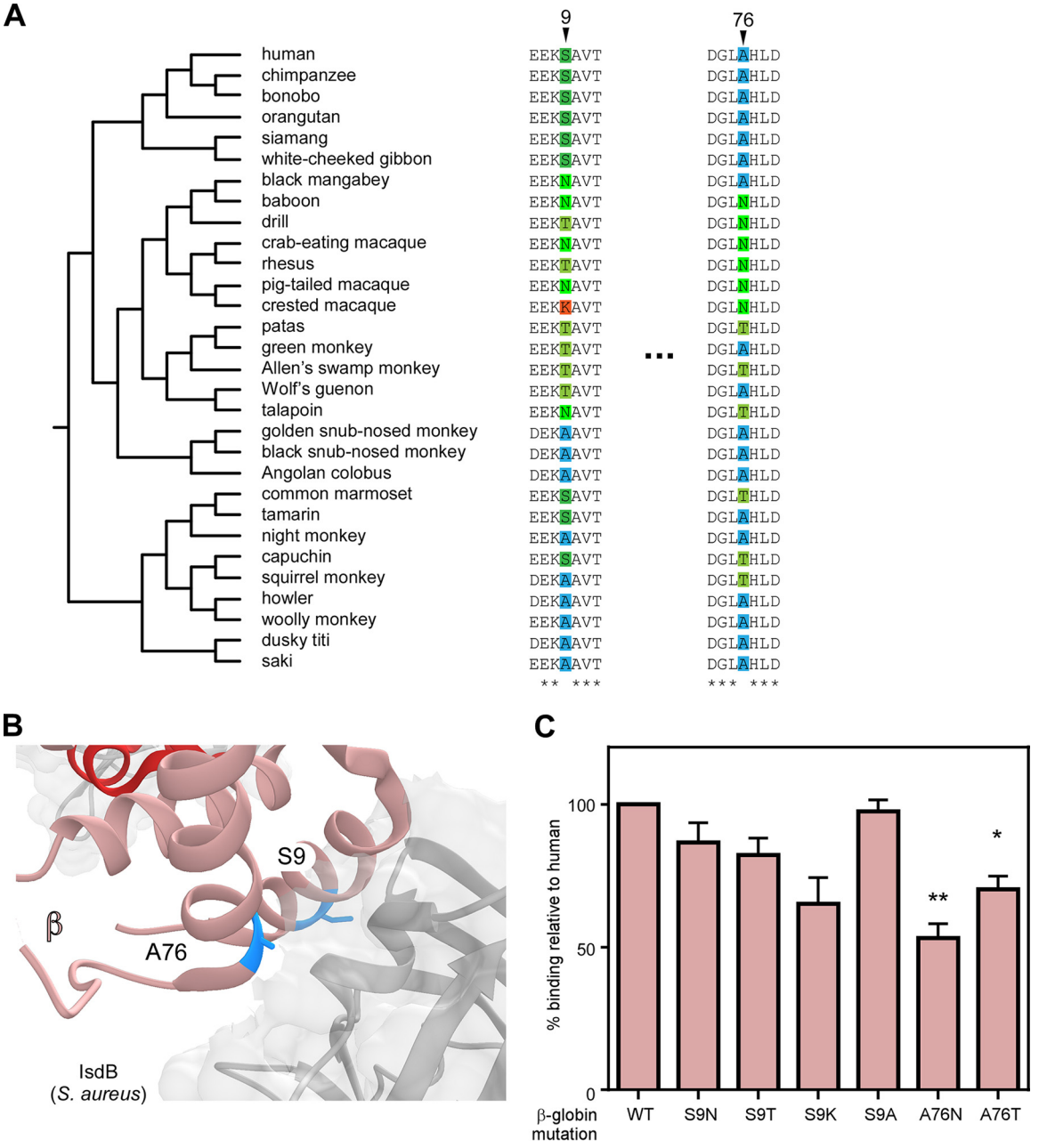

FIG 4 β-Globin divergence contributes to *S. aureus* hemoglobin binding. (A) Species phylogenies and sequence alignments surrounding positions exhibiting signatures of positive selection in β-globin. (B) Residues 9 and 76 of human β-globin (salmon) interact closely with IsdB (gray) (PDB 5VMM). (C) An iron-starved *S. aureus* wild type was incubated with purified recombinant human hemoglobin or variants of human hemoglobin encoding variants in β-globin, and bound hemoglobin was quantified. The means from four independent experiments with 3 biological replicates ± SEM are shown; *, $P < 0.05$; **, $P < 0.005$ by two-way ANOVA with Sidak's correction for multiple comparisons comparing transformed (percent value) data.

(Fig. 5A) are both primate associated and, unlike most other staphylococci, harbor IsdB. We measured the ability of IsdB from *S. argenteus* and *S. schweitzeri* to bind hemoglobin by expressing them ectopically in *S. aureus* lacking the native *isdB* gene. Consistent with their overall high sequence identity, *S. schweitzeri* and *S. argenteus* IsdB bound primate hemoglobin with a similar pattern of species preference as *S. aureus* (Fig. 5B and S6). However, both the IsdB of *S. schweitzeri* and *S. argenteus* displayed reduced binding of talapoin hemoglobin, and *S. argenteus* IsdB did not bind marmoset hemoglobin significantly less than human hemoglobin. These data indicate that the variation among IsdB sequences impacts species-specific hemoglobin capture.

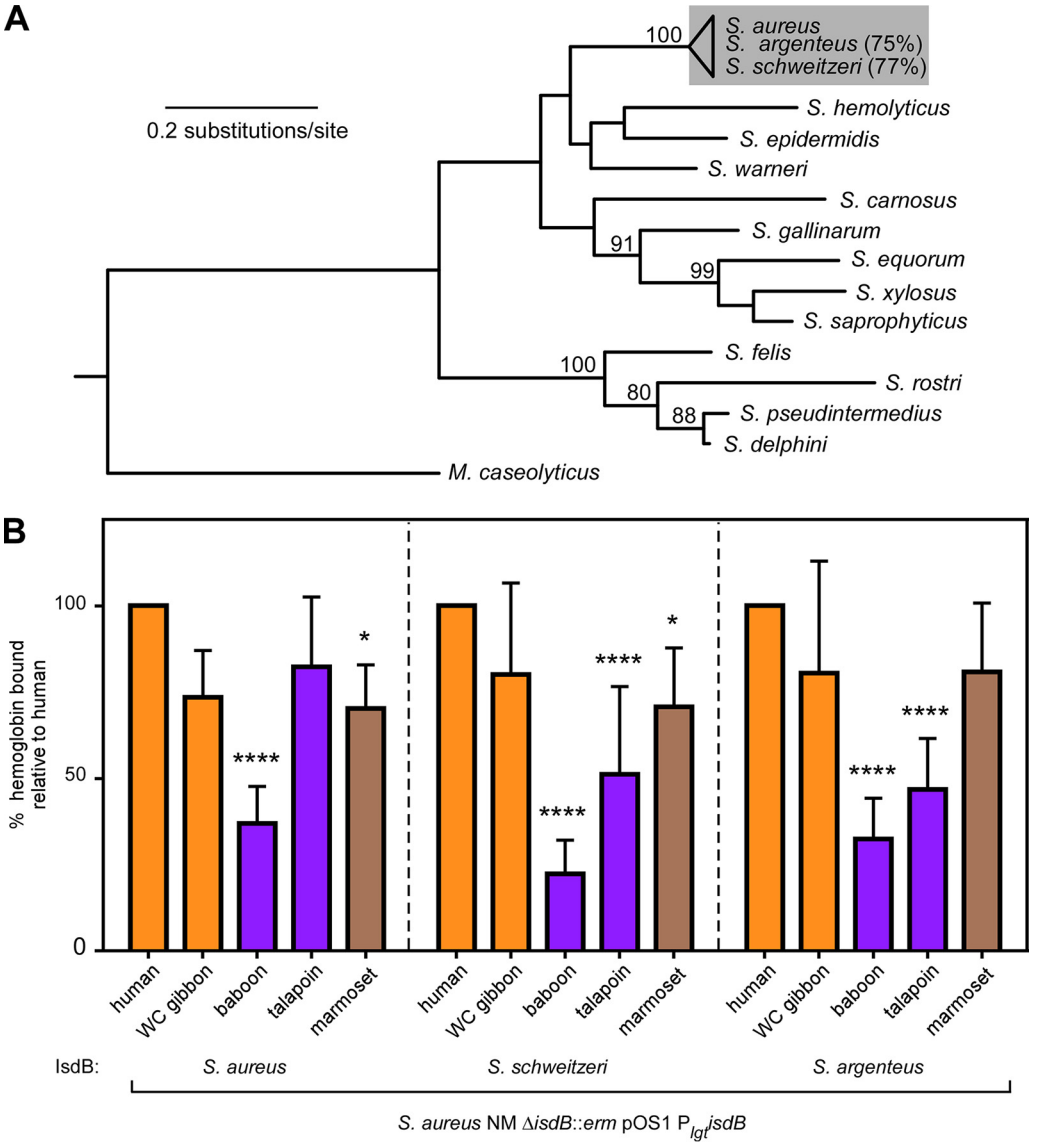

FIG 5 IsdB diversity among related staphylococcal strains impacts primate-specific hemoglobin capture. (A) Maximum likelihood phylogeny of the DNA gyrase A protein from representative staphylococci generated using PhyML. *M. caseolyticus* was included as an outgroup. The similarity of IsdB in *S. argenteus* and *S. schweitzeri* relative to *S. aureus* is shown on the right. Bootstrap values above 80 are indicated. (B) *S. aureus* lacking native *isdB* but harboring constitutively expressed plasmid-borne *isdB* variants were incubated with purified recombinant hemoglobin and from hominoid (orange), Old World monkey (purple), and New World monkeys (brown) and bound hemoglobin was quantified. The means from three independent experiments with 3 biological replicates ± SEM are shown; *, $P < 0.05$; ****, $P < 0.0001$ by two-way ANOVA with Sidak's correction for multiple comparisons, comparing transformed (percent value) data.

IsdB NEAT1 domain diversity among staphylococci modulates human hemoglobin recognition. A closer examination of the Q162R-S170T region of IsdB NEAT1 revealed variation between related staphylococci but no variation in the critical heme-binding region of NEAT2 (Fig. 6A). This region of NEAT1 closely interacts with the N-terminal helices of either α-globin or β-globin, in close proximity to both discrete sites bearing signatures of adaptive evolution in α-globin and β-globin (Fig. 6B). To determine the functional consequences of variation in this NEAT1 domain, Q162 and S170T were mutagenized in *S. aureus* IsdB to mimic the sequence of *S. schweitzeri* and *S. argenteus*. These residues are not expected to disrupt IsdB tertiary structure, as they already exist in related IsdB proteins. Variations at both of these positions reduced the affinity for human hemoglobin, showing that in the context of *S. aureus* IsdB, Q162 and

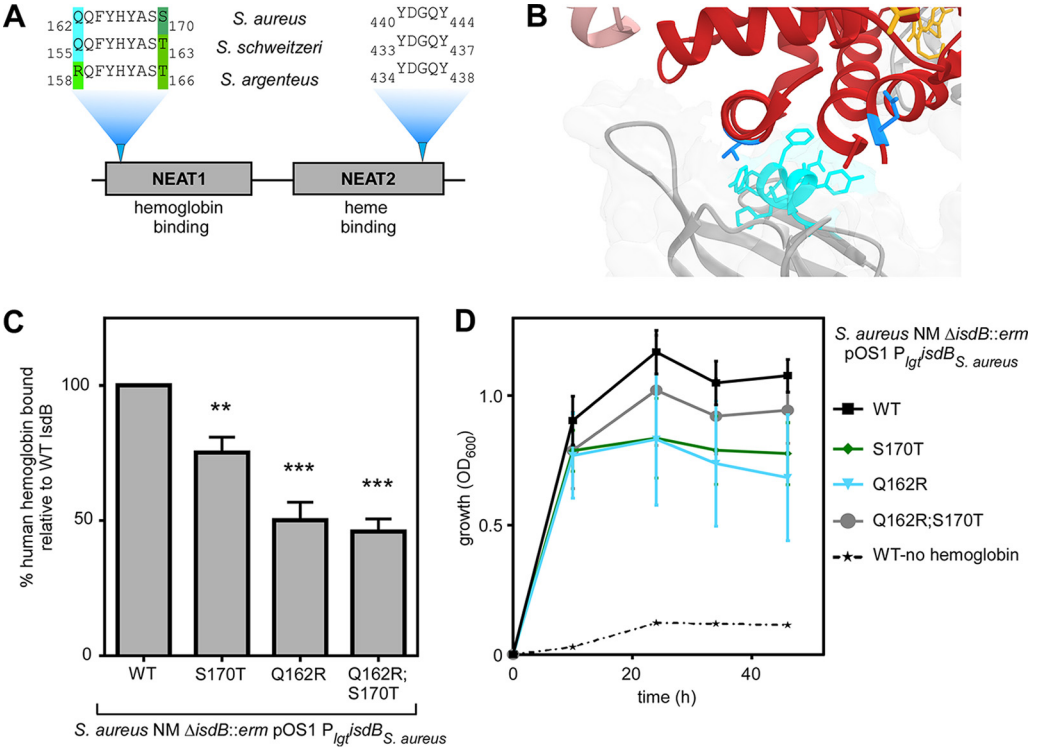

FIG 6 IsdB NEAT1 domain diversity among staphylococci modulates human hemoglobin recognition. (A) An alignment of the NEAT1 subdomain critical for hemoglobin binding shows variation among staphylococcal IsdB, while no variation was observed for the NEAT2 subdomain required for heme binding. (B) The Q162 to S170 subdomain of NEAT1 (cyan) is proximal to helices containing T8 and N78 of α-globin (red). (C) *S. aureus* lacking native *isdB* but harboring constitutively expressed plasmid-borne *S. aureus isdB* variants was incubated with purified recombinant human hemoglobin, and bound hemoglobin was quantified. (D) The growth of *S. aureus* lacking native *isdB* but harboring constitutively expressed plasmid-borne *S. aureus isdB* variants using hemoglobin as the sole iron source was monitored over time. Panel C shows, the means from three independent experiments with 3 biological replicates ± SEM; **, $P < 0.005$; ***, $P < 0.0005$ by two-way ANOVA with Sidak's correction for multiple comparisons, comparing transformed (percent value) data. Panel D shows the results of two independent experiments with six biological replicates each ± standard deviations.

S170 are required for high-affinity hemoglobin binding (Fig. 6C and S7). Additionally, mutagenized IsdB failed to fully support the growth of *S. aureus* using human hemoglobin as the sole iron source (Fig. 6D), which supports the conclusion that this NEAT1 subdomain of *S. aureus* has evolved for optimal binding and utilization of human hemoglobin.

DISCUSSION

In this work, we report that recurrent positive selection acting on primate α- and β-globin proteins restricts hemoglobin binding and nutrient acquisition by pathogenic *S. aureus*. Estimations of divergence in the *Staphylococcus* genus have been lacking; however, the Kloos hypothesis (41) contends that staphylococci have coevolved with their mammalian hosts over long evolutionary timescales. In support of this concept, primate specificity among staphylococci has been reported, including *S. aureus*, *S. epidermidis*, and *S. warneri*, as well as avian (*S. gallinarum*), equine (*S. equorum*), and other taxa. Indeed, it has been proposed that the canine-associated *S. pseudintermedius* diverged from *S. aureus* simultaneously with the divergence of Primate and Carnivora orders (42). Most staphylococci are commensal organisms, while *S. aureus* is uniquely adapted to infect deep tissue and cause disease. As such, the IsdB system is only harbored by *S. aureus* and closely related primate-associated staphylococci. By narrowing our analysis of hemoglobin evolution to primates, we were thus able to assess specific biological features of primate-associated staphylococci.

An outstanding question in the study of *S. aureus* evolution has been determining the selective pressures responsible for human-specific virulence factors. *S. aureus*

asymptomatically colonizes the anterior nares of approximately one-third of the human population yet is capable of causing a wide range of invasive diseases. While some bacterial colonization factors have been implicated in the pathogenesis, many virulence factors have evolved highly specific targets that are not obviously involved in nasal colonization (43). As such, we cannot definitively conclude that IsdB evolution has been driven by selection during invasive disease. It is also likely that variation across IsdB sequences of *S. aureus*, *S. argenteus*, and *S. schweitzeri* may be the results of antigenic variation to evade the immune system. By focusing on the hemoglobin binding pocket of IsdB, we have been able to pinpoint critical variations for hemoglobin specificity.

Our phylogenetic analyses revealed strikingly parallel signatures of positive selection between the α- and β-globin genes across primates. In particular, rapidly evolving sites in the α- and β-globin A-helices are predicted to be homologous on the basis of the predicted protein alignments. Our results suggest that these correlations reflect selection in response to NEAT domain-containing bacterial receptors like IsdB with conserved globin-binding sites. A well-established body of literature has shown that other selective pressures play important roles in the patterns of hemoglobin polymorphism and divergence across vertebrates, including the adaptation to high altitude and malaria resistance (34, 38). It is therefore possible that the signatures of selection detected in our study were driven by pressures other than nutritional immunity. Nonetheless, our empirical results demonstrate that variation in hemoglobins at discrete sites has important functional consequences for bacterial iron acquisition.

Previous studies have illustrated how mutations in hemoglobin coding or regulatory regions can have highly deleterious effects on heme binding, oxygen affinity, and protein stability (44, 45). In addition to aforementioned sickle-cell alleles, dozens of hemoglobin mutations in humans have been reported that contribute to genetic disease, including anemia and thalassemia (46). Thus, despite identifying particular sites that are highly divergent among primates, much of the globin gene content is constrained due to purifying selection. In future work, it would be useful to determine how variation among primate globins impacts other biochemical functions, including heme binding and oxygen affinity. Such insights might improve our fundamental understanding of hemoglobin biology and the mechanisms underlying human hemoglobinopathies.

In conclusion, this work illustrates how rapid site-specific hemoglobin variation restricts heme acquisition by the prominent human pathogen *S. aureus*. These findings provide a fundamental new perspective on vertebrate globin evolution, highlighting nutritional immunity as a selective pressure that might strongly impact divergence and natural selection. Future studies will assist in illuminating how these combinations of adaptive mutations contribute to hemoglobin function and host physiology. An understanding of the genetic and molecular determinants of bacterial pathogenicity is critical for developing new antimicrobial treatment strategies, particularly as major pathogens such as *S. aureus* continue to develop resistance to existing antibiotics. Combining comparative genetics with molecular experimentation in turn provides not only a historical perspective of host-microbe evolutionary conflict but also mechanistic insights on modern human infectious disease.

MATERIALS AND METHODS

Bacterial strains. The bacterial strains and plasmids used in this study are listed in Table 1. For *Escherichia coli* strains, LB agar and broth (Fisher, Hampton, NH) were routinely used, and growth was at 37°C. For the selection of pHUG21, 12.5 μg/ml of carbenicillin (Fisher) was used, for the selection of pHb0.0, 5 μg/ml of tetracycline hydrochloride (Alfa Aesar, Haverhill, MA) was used, and for the selection of pOS1 P_{lgt}, 50 μg/ml of carbenicillin was used. *Staphylococcus* strains were grown at 37°C using tryptic soy agar and broth (Fisher), except where noted throughout. For the selection of pOS1 P_{lgt}, 10 μg/ml chloramphenicol (Fisher) was used except where noted. The strains were streaked onto agar from stocks stored at −80°C 2 days prior to each experiment.

Hemoglobin cloning and genetic manipulation. We compiled a subset of α- and β-globin sequences from GenBank, as well as cloned α-globin orthologs from cDNA derived from primate cell lines and β-globin orthologs from primate genomic DNA. Hemoglobin gene sequences have been deposited in GenBank (accession numbers MH382883 to MH382906). Hemoglobin gene sequences obtained from GenBank include those for olive baboon, bonobo, white-headed capuchin, chimpanzee, Angolan colo-

TABLE 1 Strains and plasmids

Strain or plasmid	Source and/or reference
Strains	
Escherichia coli DH5α	Laboratory stock, Thermo Fisher
Escherichia coli BL21(DE3) pHUG21	Douglas Henderson (University of Texas of the Permian Basin); 52
Staphylococcus aureus RN4220	53
S. aureus Newman	Laboratory stock; 54
S. aureus Newman Δ*isdB*::*erm*	7
S. argenteus MSHR1132	DSMZ
S. schweitzeri FSA084	DSMZ
Plasmids	Source
pHb0.0-human	John Olson (Rice University); 52
pHb0.0-white-cheeked gibbon	This paper
pHb0.0-baboon	This paper
pHb0.0-talapoin	This paper
pHb0.0-marmoset	This paper
pHb0.0-alpha$_{human}$beta$_{baboon}$	This paper
pHb0.0-alpha$_{baboon}$beta$_{human}$	This paper
pHb0.0-human αT8K	This paper
pHb0.0-human αA5D;T8K;N9H	This paper
pHb0.0-human αN78Q	This paper
pHb0.0-human αN78H	This paper
pHb0.0-human βS9N	This paper
pHb0.0-human βS9T	This paper
pHb0.0-human βS9K	This paper
pHb0.0-human βS9A	This paper
pHb0.0-human βA76N	This paper
pHb0.0-human βA76T	This paper
pOS1 P$_{lgt}$	55
pOS1 P$_{lgt}$*isdB*$_{aureus}$	This paper
pOS1 P$_{lgt}$*isdB*$_{schweitzeri}$	This paper
pOS1 P$_{lgt}$*isdB*$_{argenteus}$	This paper
pOS1 P$_{lgt}$*isdB*$_{aureus}$ Q162R	This paper
pOS1 P$_{lgt}$*isdB*$_{aureus}$ S170T	This paper
pOS1 P$_{lgt}$*isdB*$_{aureus}$ Q162R;S170T	This paper

bus, northern white-cheeked gibbon, green monkey, human, drill, crab-eating macaque, common marmoset, Sumatran orangutan, rhesus macaque, black snub-nosed monkey, golden snub-nosed monkey, and squirrel monkey. Primate cell lines were purchased from the Coriell Institute for Medical Research (Camden, NJ). The α-globin orthologs cloned from cDNA (with Coriell identifier [ID] numbers) are as follows: African green monkey (PR01193), black-and-white colobus (PR00240), white-handed gibbon (PR01131), Western lowland gorilla (AG05251), Francois' leaf monkey (PR01099), black crested mangabey (PR01215), white-faced marmoset (PR00789), Nancy Ma's night monkey (PR00627), patas monkey (AG06116), proboscis monkey, Allen's swamp monkey (PR01231), talapoin (PR00716), and Wolf's guenon (PR00486). The β-globin orthologs cloned from genomic DNA (with Coriell ID numbers) are as follows: crested macaque (PR01215), Bolivian red howler monkey (PR00708), pigtailed macaque, black-crested mangabey (PR01215), Nancy Ma's night monkey(PR00627), patas monkey (AG06116), white-faced saki (PR00239), island siamang (PR00722), Allen's swamp monkey (PR01231), talapoin (PR00716), Spix's saddle-back tamarin (AG05313), dusky titi (PR00742), Wolf's guenon (PR00486), and common woolly monkey (PR00525).

Primate hemoglobin cDNA was cloned into pHb0.0 using Gibson assembly (New England Biolabs [NEB], Ipswich, MA). In general, each α- and β-globin gene cDNA was amplified from the template (above) using Phusion 2$\times$ master mix (Thermo, Waltham, MA) with primers that also had homology to pHb0.0. All primers are listed in Table S1 in the supplemental material. Because of cDNA sequence homology, some primers were used for multiple species. pHb0.0-human was digested with PacI (NEB) and HindIII-HF (NEB), and the doubly digested vector was isolated by gel purification (Qiagen, Germantown, MD). PCR products were assembled with digested pHb0.0, transformed to DH5α, reisolated with a Mini-prep (Thermo), and confirmed by sequencing (GeneWiz, South Plainfield, NJ) with primers pHb0.0_for/pHb0.0_rev. Globin cDNA was amplified with the following primers for Gibson assembly: white-cheeked gibbon α-globin, primers AF327/328; white-cheeked gibbon β-globin, primers AF329/330; baboon α-globin, primers AF331/332; baboon β-globin, primers AF329/330; talapoin α-globin, primers AF327/328; talapoin β-globin, primers AF329/330; marmoset α-globin, primers AF333/334; and marmoset β-globin, primers AF329/335.

Chimeric hemoglobins were prepared by subcloning the α-globins. To enable digestion with XbaI (NEB) (which is sensitive to *dam* methylation) pHb0.0-human and pHb0.0-baboon were transformed and reisolated from *E. coli* K1077 (Δ*dam* Δ*dcm*). The α-globin from each plasmid was excised by digestion

with XbaI (NEB) and PacI (NEB), and the α-globin and doubly digested pHb0.0 containing β-globin were separately isolated by gel purification (Qiagen). Human α-globin was ligated into pHb0.0 containing baboon β-globin and baboon α-globin was ligated (T4 ligase; NEB) into pHb0.0 containing human β-globin. The chimeras were confirmed by sequencing (GeneWiz) with primers pHb0.0_for/pHb0.0_rev.pHb0.0-human was mutagenized using a QuikChange site-directed mutagenesis kit (Agilent, Santa Clara, CA) to create changes in the α-gene: T8K (primers AF289/290), T8K/N9H (primers JC112/113; using pHb0.0-human αT8K as the template), A5D/T8K/N9H (primers JC114/115; using pHb0.0-human αT8K;N9H as the template), N78Q (primers AF291/292), and N78H (primers AF293/294). Changes in the human β-gene were as follows: S9N (primers AF303/304), S9T (primers AF307/308), S9A (primers AF309/310), S9K (primers AF305/306), A76N (primers AF313/314), and A76T (primers AF311/312).

Phylogenetic analyses. Hemoglobin DNA sequence alignments were performed using MUSCLE. Input phylogenies were based upon supported species relationships (47) as well as maximum likelihood gene phylogenies generated using PhyML with SPR topology search and 1,000 bootstraps for branch support (48). Tests for positive selection were performed using codeml from the PAML software package with the F3X4 codon frequency model. Likelihood ratio tests (LRTs) were performed by comparing pairs of site-specific models (NS sites): M1 (neutral) with M2 (selection), M7 (neutral, beta distribution of $dN/dS < 1$) with M8 (selection, beta distribution, $dN/dS > 1$ allowed). Additional tests which also account for synonymous rate variation and recombination, including FUBAR, FEL, and MEME, were performed using the HyPhy software package via the Datamonkey server (49, 50). Sites under positive selection were mapped onto three-dimensional molecular structures by using Chimera (51) (http://www.cgl.ucsf.edu/chimera/).

The staphylococcal DNA gyrase gene tree was generated using PhyML with 1,000 bootstraps as described above. *Macrococcus caseolyticus* DNA gyrase was included as an outgroup. The similarity of IsdB sequences in *S. argenteus* and *S. schweitzeri* relative to that in *S. aureus* is shown in Fig. 5.

Recombinant purification of hemoglobin. Hemoglobin expression strains [BL21(DE3) pHUG21 pHb0.0] were streaked onto LB agar containing 12.5 μg/ml carbenicillin and 5 μg/ml tetracycline hydrochloride. pHb0.0 harbors both α- and β-globin genes, and proper folding and tetramerization require sufficient intracellular heme. Therefore, pHUG21, which encodes a heme uptake system, is coexpressed, and hemin is supplemented in the medium (52). Single colonies were inoculated in 5 ml of LB broth supplemented with 12.5 μg/ml carbenicillin and 5 μg/ml tetracycline hydrochloride and grown for 14 h at 37°C with shaking. This culture was used for inoculating 1:500 into 1.5 liters of LB with 12.5 μg/ml carbenicillin, 5 μg/ml tetracycline hydrochloride, 100 μM hemin (prepared fresh at 10 mM in 0.1 M NaOH; Sigma, St. Louis, MO), and 50 μg/ml of the iron chelator ethylenediamine-di(*o*-hydroxyphenylacetic acid (EDDHA, solid added directly to medium; LGC Standards, Teddington, UK;) in a 2.8-liter Fernbach flask. Cultures were grown at 37°C until the optical density at 600 nm (OD_{600}) reached 0.6 to 0.8. The expression of hemoglobin was induced with 40 μg/ml IPTG (isopropyl-β-isopropyl-β-D-thiogalactopyranoside-thiogalactopyranoside; RPI, Mount Prospect, IL). At 16 h postinduction at 37°C, cells were collected by centrifugation. The cell pellet was resuspended in 20 ml phosphate-buffered saline (PBS) containing 10 mM imidazole (Fisher), 5 mM $MgCl_2$ (Sigma), 1 Roche protease inhibitor tablet (Fisher), approximately 1 mg/ml of lysozyme (Thermo), and 100 μg/ml DNase from bovine pancreas (Sigma). The cell pellet resuspended with rocking for 20 min at room temperature after incubating on ice for 20 min. The cells were lysed using an Emulsiflex (Avestin, Ottawa, CA), and then the cell lysate was clarified by ultracentrifugation (60 min at 17,000 × g). The cell lysate was applied to a 3 ml of nickel-nitrilotriacetic acid (Ni-NTA) resin (Qiagen) in a gravity column, to which hemoglobin binds, and washed with 50 ml PBS containing 10 mM imidazole. Hemoglobin was eluted with 6 ml PBS containing 500 mM imidazole, with the first 1 ml of eluate discarded. The hemoglobin-containing eluate was dialyzed twice sequentially in PBS at 4°C. Purified hemoglobin was filter sterilized with a 0.45-μm filter and stored in aliquots in liquid nitrogen. The hemoglobin concentration was measured with Drabkin's reagent (Sigma) using human hemoglobin as a standard, ranging from 2 to 6 mg/ml. The relative purity was assessed using SDS-PAGE before use in experiments, as shown in Fig. S8.

Whole-cell hemoglobin binding assay. *S. aureus* strains were streaked on tryptic soy agar (containing 10 μg/ml chloramphenicol for strains carrying plasmids) and grown at 37°C for 24 h. Single colonies were used to inoculate 3 ml of RPMI containing 1% Casamino Acids and 0.5 mM 2,2′-dipyridyl (Acros/Fisher) to induce the expression of chromosomal *isdB* or 10 μg/ml chloramphenicol (for strains carrying plasmids with constitutive *isdB* expression). After 14 to 16 h of growth at 37°C with shaking, 2 OD_{600} units (except for experiments shown in part in Fig. 3D and S4C, where 1 OD_{600} unit was used) were collected by centrifugation in a 1.5-ml Eppendorf tube. The cell pellet was resuspended with 1 ml PBS or PBS containing recombinant hemoglobin. Then, 10 μg/ml (chromosomal *isdB*) or 2.5 μg/ml (plasmid-borne *isdB*) of hemoglobin was used. The cells were incubated with hemoglobin or PBS for 30 min at 37°C with shaking, and then the cells were collected by centrifugation at 4°C at 8,000 × *g*. Cells were washed thrice by pipetting with 1 ml ice-cold PBS and centrifuging at 4°C at 8,000 × *g*. After the final wash, the cells were resuspended in 30 μl 0.5 M Tris (pH 8.0; Fisher) containing 4% SDS (Fisher) and heated at 90°C for 5 min to remove surface-bound proteins. The cells were collected by centrifugation at 8,000 × *g*, and the eluate was added to 6× loading buffer and heated at 90°C for 5 min. The samples were subjected to 12% or 17.5% SDS-PAGE and silver stained (GE, Boston, MA). The gels were imaged using an Alpha Innotech Alpha Imager or Bio-Rad ChemiDoc MP imaging system. Quantification was performed by densitometric analysis with Image J (NIH) according to the software instructions and by quantifying the area under the peak that corresponds to the hemoglobin band, excluding background density. Because of the variation in stain intensity and quantity of nonspecific bands across gels, all comparisons were made

within the same gel, and the relative density was calculated for each biological replicate within the same gel; the comparison was either to human hemoglobin or wild-type IsdB, depending on the assay. Additionally, PBS-only samples and *S. aureus* Δ*isdB*::*erm* were used to verify that hemoglobin binding in this assay is IsdB dependent (Fig. S4C, S5, and S8) as previously observed, and that recombinant human hemoglobin is bound equally as well as hemoglobin purified from human blood (Fig. S1) (11, 13).

Growth with hemoglobin as sole iron source. For hemoglobin variants (Fig. 2D and S3), *S. aureus* Newman WT was streaked onto tryptic soy agar and allowed to grow for 24 h at 37°C. A few colonies were used to inoculate 5 ml of RPMI (Corning, Corning, NY) supplemented with 1% Casamino Acids (Fisher) and 0.5 mM EDDHA (prepared fresh in ethanol). After growth to stationary phase at 37°C with shaking, approximately 16 h, 4 μl of culture was inoculated in 196 μl of medium in a 96-well plate, and the OD_{600} at 37°C with shaking was monitored over time using a BioTek plate reader. The medium was RPMI containing 1% Casamino Acids that had been depleted of cations with Chelex 100 (Sigma) according to the manufacturer's instructions, filter sterilized, and supplemented with 25 μM $ZnCl_2$, 25 μM $MnCl_2$, 100 μM $CaCl_2$, and 1 mM $MgCl_2$ (all from Fisher) to restore noniron cations, 1.5 mM EDDHA to chelate any remaining free iron, and 2.5 μg/ml of recombinant purified hemoglobin as the sole iron source.

For IsdB variants (Fig. 6D), *S. aureus* strains were streaked onto tryptic soy agar containing 10 μg/ml chloramphenicol and allowed to grow for 24 h at 37°C. A single colony was resuspended in 120 μl RPMI containing 1 μM EDDHA (prepared fresh in 0.1 M NaOH) and 5 μg/ml chloramphenicol. Then, 100 μl was added to 2 ml of RPMI containing 1 μM EDDHA and 5 μg/ml chloramphenicol and grown at 37° with shaking in aeration tubes for 8 h. The OD_{600} was measured for each culture and normalized to 1, and 5 μl was used to inoculate 2 ml of RPMI containing 1 μM EDDHA, 5 μg/ml chloramphenicol, and 50 nM hemoglobin or no hemoglobin (for Δ*isdB* pOS1 P_{lgt}*isdB*). Growth was monitored every 12 h by removing 50 μl of culture and adding to 150 μl PBS to measure the OD_{600} with path length correction in a BioTek plate reader, with the background subtracted from the corrected OD_{600} values. Growth using hemoglobin as a sole iron source in both assays is IsdB dependent (11, 13, 22).

Cloning of *isdB*. The full-length coding sequences of IsdB were amplified from genomic DNA using Phusion 2× high-fidelity master Mix (Thermo); cells were treated with 20 μg of lysostaphin (AMBI Products, Lawrence, NY), and DNA was isolated with a Wizard genomic DNA extraction kit (Promega, Madison, WI). *S. aureus isdB* (*NWMN_1040*) was amplified using primers JC343/344, *S. schweitzeri isdB* (*ERS140239_01018*) using primers JC218/219, and *S. argenteus isdB* (*SAMSHR1132_09750*) using primers JC216/217. Each primer pair included homology to pOS1 P_{lgt} digested with NdeI and BamHI-HF (NEB), and PCR products were ligated to pOS1 P_{lgt} with Hi-Fi assembly (NEB), transformed into *E. coli* DH5α, and reisolated with a Mini-prep (Thermo). All plasmids were sequence confirmed by Sanger sequencing (GeneWiz). Plasmids were transformed into RN4220 by electroporation, reisolated, and transformed into *S. aureus* Newman Δ*isdB*::*erm* by electroporation.

***S. aureus* IsdB site-directed mutagenesis.** pOS1 P_{lgt}*isdB*$_{aureus}$ was subjected to site-directed mutagenesis by PCR with a Q5 site-directed mutagenesis kit (NEB). Primer pairs with desired mutation were used to create Q162R (primers JC315/316), S170T (primers 317/318) and Q162R;S170T (primers JC319/320). PCR products were transformed to DH5α. Plasmids were isolated and subjected to Sanger sequencing with primers JC228/229 (GeneWiz) to identify successful incorporation of the desired mutation. Plasmids were transformed into RN4220 by electroporation, reisolated, and transformed into *S. aureus* Newman Δ*isdB*::*erm* by electroporation.

Quantification and statistical analysis. Specific statistical details for each experiment can be found in the corresponding figure legends. Data analysis and statistical tests were performed in Prism 6 (GraphPad).

SUPPLEMENTAL MATERIAL

Supplemental material for this article may be found at https://doi.org/10.1128/mBio.01524-18.

DATA SET S1, XLSX file, 0.03 MB.
FIG S1, TIF file, 1.1 MB.
FIG S2, TIF file, 1.9 MB.
FIG S3, TIF file, 1.3 MB.
FIG S4, TIF file, 2.3 MB.
FIG S5, TIF file, 2.8 MB.
FIG S6, TIF file, 2 MB.
FIG S7, TIF file, 1.4 MB.
FIG S8, TIF file, 2 MB.
TABLE S1, DOCX file, 0.01 MB.

ACKNOWLEDGMENTS

We thank members of the Skaar and Barber laboratories for critical evaluation of the manuscript. We acknowledge the gift of pHUG21 from Douglas Henderson (University of Texas of the Permian Basin) and pHb0.0 from John Olson (Rice University).

Work in E.P.S. laboratory was supported by National Institutes of Health (NIH) grants R01AI069233 and R01AI073843. Work in M.F.B laboratory was supported by NIH grants R00GM115822 and U54DK110858-02 (subaward 10040500-22) and a Faculty Scholar Award from the Donald E. and Delia B. Baxter Foundation. J.E.C. was supported by NIH grants T32GM065086 and F31AI126662.

Conceptualization, J.E.C., E.P.S., and M.F.B.; investigation, J.E.C., H.B.B., A.J.F., and M.F.B.; writing of the original draft, J.E.C., E.P.S., and M.F.B.; writing, reviewing, and editing, J.E.C., H.B.B., A.J.F., E.P.S., and M.F.B.; visualization, J.E.C., and M.F.B.; supervision, E.P.S. and M.F.B.; funding acquisition, E.P.S. and M.F.B. The authors declare no competing interests.

ADDENDUM IN PROOF

While our article was in press, a complementary article was published by A. Mozzi et al. (Front Immunol 9:2086, 2018, https://doi.org/10.3389/fimmu.2018.02086).

REFERENCES

1. Palmer LD, Skaar EP. 2016. Transition metals and virulence in bacteria. Annu Rev Genet 50:67–91. https://doi.org/10.1146/annurev-genet-120215-035146.
2. Weinberg ED. 1975. Nutritional immunity: host's attempt to withhold iron from microbial invaders. JAMA 231:39–41. https://doi.org/10.1001/jama.1975.03240130021018.
3. Schade AL, Caroline L. 1944. Raw hen egg white and the role of iron in growth inhibition of *Shigella dysenteriae*, *Staphylococcus aureus*, *Escherichia coli* and *Saccharomyces cerevisiae*. Science 100:14–15. https://doi.org/10.1126/science.100.2584.14.
4. Cassat JE, Skaar EP. 2013. Iron in infection and immunity. Cell Host Microbe 13:509–519. https://doi.org/10.1016/j.chom.2013.04.010.
5. Choby JE, Skaar EP. 2016. Heme synthesis and acquisition in bacterial pathogens. J Mol Biol 428:3408–3428. https://doi.org/10.1016/j.jmb.2016.03.018.
6. Klevens RM, Morrison MA, Nadle J, Petit S, Gershman K, Ray S, Harrison LH, Lynfield R, Dumyati G, Townes JM, Craig AS, Zell ER, Fosheim GE, McDougal LK, Carey RB, Fridkin SK. 2007. Invasive methicillin-resistant *Staphylococcus aureus* infections in the United States. JAMA 298:1763–1771. https://doi.org/10.1001/jama.298.15.1763.
7. Mazmanian SK, Skaar EP, Gaspar AH, Humayun M, Gornicki P, Jelenska J, Joachmiak A, Missiakas DM, Schneewind O. 2003. Passage of heme-iron across the envelope of *Staphylococcus aureus*. Science 299:906–909. https://doi.org/10.1126/science.1081147.
8. Spaan AN, Reyes-Robles T, Badiou C, Cochet S, Boguslawski KM, Yoong P, Day CJ, de Haas CJC, van Kessel KPM, Vandenesch F, Jennings MP, Le Van Kim C, Colin Y, van Strijp JAG, Henry T, Torres VJ. 2015. *Staphylococcus aureus* targets the duffy antigen receptor for chemokines (DARC) to lyse erythrocytes. Cell Host Microbe 18:363–370. https://doi.org/10.1016/j.chom.2015.08.001.
9. Torres VJ, Pishchany G, Humayun M, Schneewind O, Skaar EP. 2006. *Staphylococcus aureus* IsdB is a hemoglobin receptor required for heme iron utilization. J Bacteriol 188:8421–8429. https://doi.org/10.1128/JB.01335-06.
10. Dryla A, Gelbmann D, Von Gabain A, Nagy E. 2003. Identification of a novel iron regulated staphylococcal surface protein with haptoglobin-haemoglobin binding activity. Mol Microbiol 49:37–53. https://doi.org/10.1046/j.1365-2958.2003.03542.x.
11. Pishchany G, Sheldon JR, Dickson CF, Alam MT, Read TD, Gell DA, Heinrichs DE, Skaar EP. 2014. IsdB-dependent hemoglobin binding is required for acquisition of heme by *Staphylococcus aureus*. J Infect Dis 209:1764–1772. https://doi.org/10.1093/infdis/jit817.
12. Cheng AG, Kim HK, Burts ML, Krausz T, Schneewind O, Missiakas DM. 2009. Genetic requirements for *Staphylococcus aureus* abscess formation and persistence in host tissues. FASEB J 23:3393–3404. https://doi.org/10.1096/fj.09-135467.
13. Pishchany G, McCoy AL, Torres VJ, Krause JC, Crowe JE, Fabry ME, Skaar EP. 2010. Specificity for human hemoglobin enhances *Staphylococcus aureus* infection. Cell Host Microbe 8:544–550. https://doi.org/10.1016/j.chom.2010.11.002.
14. Malachowa N, Whitney AR, Kobayashi SD, Sturdevant DE, Kennedy AD, Braughton KR, Shabb DW, Diep BA, Chambers HF, Otto M, DeLeo FR. 2011. Global changes in *Staphylococcus aureus* gene expression in human blood. PLoS One 6:e18617. https://doi.org/10.1371/journal.pone.0018617.
15. Fowler VG, Jr, Proctor RA. 2014. Where does a *Staphylococcus aureus* vaccine stand? Clin Microbiol Infect 20 Suppl 5:66–75. https://doi.org/10.1111/1469-0691.12570.
16. Muryoi N, Tiedemann MT, Pluym M, Cheung J, Heinrichs DE, Stillman MJ. 2008. Demonstration of the iron-regulated surface determinant (Isd) heme transfer pathway in *Staphylococcus aureus*. J Biol Chem 283:28125–28136. https://doi.org/10.1074/jbc.M802171200.
17. Skaar EP, Gaspar AH, Schneewind O. 2004. IsdG and IsdI, heme-degrading enzymes in the cytoplasm of *Staphylococcus aureus*. J Biol Chem 279:436–443. https://doi.org/10.1074/jbc.M307952200.
18. Grigg JC, Vermeiren CL, Heinrichs DE, Murphy ME. 2007. Heme coordination by *Staphylococcus aureus* IsdE. J Biol Chem 282:28815–28822. https://doi.org/10.1074/jbc.M704602200.
19. Zhu H, Xie G, Liu M, Olson JS, Fabian M, Dooley DM, Lei B. 2008. Pathway for heme uptake from human methemoglobin by the iron-regulated surface determinants system of *Staphylococcus aureus*. J Biol Chem 283:18450–18460. https://doi.org/10.1074/jbc.M801466200.
20. Reniere ML, Ukpabi GN, Harry SR, Stec DF, Krull R, Wright DW, Bachmann BO, Murphy ME, Skaar EP. 2010. The IsdG-family of haem oxygenases degrades haem to a novel chromophore. Mol Microbiol 75:1529–1538. https://doi.org/10.1111/j.1365-2958.2010.07076.x.
21. Skaar EP, Humayun M, Bae T, DeBord KL, Schneewind O. 2004. Iron-source preference of *Staphylococcus aureus* infections. Science 305:1626–1628. https://doi.org/10.1126/science.1099930.
22. Bowden CFM, Chan ACK, Li EJW, Arrieta AL, Eltis LD, Murphy MEP. 2018. Structure-function analyses reveal key features in *Staphylococcus aureus* IsdB-associated unfolding of the heme-binding pocket of human hemoglobin. J Biol Chem 293:177–190. https://doi.org/10.1074/jbc.M117.806562.
23. Daugherty MD, Malik HS. 2012. Rules of engagement: molecular insights from host-virus arms races. Annu Rev Genet 46:677–700. https://doi.org/10.1146/annurev-genet-110711-155522.
24. Hughes AL, Nei M. 1988. Pattern of nucleotide substitution at major histocompatibility complex class I loci reveals overdominant selection. Nature 335:167–170. https://doi.org/10.1038/335167a0.
25. Hamilton WD, Axelrod R, Tanese R. 1990. Sexual reproduction as an adaptation to resist parasites (a review). Proc Natl Acad Sci U S A 87:3566–3573.
26. Yang Z, Bielawski JP. 2000. Statistical methods for detecting molecular adaptation. Trends Ecol Evol 15:496–503. https://doi.org/10.1016/S0169-5347(00)01994-7.
27. Nei M, Gojobori T. 1986. Simple methods for estimating the numbers of synonymous and nonsynonymous nucleotide substitutions. Mol Biol Evol 3:418–426. https://doi.org/10.1093/oxfordjournals.molbev.a040410.
28. Demogines A, Farzan M, Sawyer SL. 2012. Evidence for ACE2-utilizing coronaviruses (CoVs) related to severe acute respiratory syndrome CoV in bats. J Virol 86:6350–6353. https://doi.org/10.1128/JVI.00311-12.
29. Sawyer SL, Wu LI, Emerman M, Malik HS. 2005. Positive selection of

primate TRIM5alpha identifies a critical species-specific retroviral restriction domain. Proc Natl Acad Sci U S A 102:2832–2837. https://doi.org/10.1073/pnas.0409853102.
30. Elde NC, Child SJ, Geballe AP, Malik HS. 2009. Protein kinase R reveals an evolutionary model for defeating viral mimicry. Nature 457:485–489. https://doi.org/10.1038/nature07529.
31. Enard D, Cai L, Gwennap C, Petrov DA. 2016. Viruses are a dominant driver of protein adaptation in mammals. Elife 5:e12469. https://doi.org/10.7554/eLife.12469.
32. Barber MF, Elde NC. 2014. Escape from bacterial iron piracy through rapid evolution of transferrin. Science 346:1362–1366. https://doi.org/10.1126/science.1259329.
33. Barber MF, Kronenberg Z, Yandell M, Elde NC. 2016. Antimicrobial functions of lactoferrin promote genetic conflicts in ancient primates and modern humans. PLoS Genet 12:e1006063. https://doi.org/10.1371/journal.pgen.1006063.
34. Storz JF, Moriyama H. 2008. Mechanisms of hemoglobin adaptation to high altitude hypoxia. High Alt Med Biol 9:148–157. https://doi.org/10.1089/ham.2007.1079.
35. Galen SC, Natarajan C, Moriyama H, Weber RE, Fago A, Benham PM, Chavez AN, Cheviron ZA, Storz JF, Witt CC. 2015. Contribution of a mutational hot spot to hemoglobin adaptation in high-altitude Andean house wrens. Proc Natl Acad Sci U S A 112:13958–13963. https://doi.org/10.1073/pnas.1507300112.
36. Natarajan C, Hoffmann FG, Weber RE, Fago A, Witt CC, Storz JF. 2016. Predictable convergence in hemoglobin function has unpredictable molecular underpinnings. Science 354:336–339. https://doi.org/10.1126/science.aaf9070.
37. Storz JF, Sabatino SJ, Hoffmann FG, Gering EJ, Moriyama H, Ferrand N, Monteiro B, Nachman MW. 2007. The molecular basis of high-altitude adaptation in deer mice. PLoS Genet 3:e45. https://doi.org/10.1371/journal.pgen.0030045.
38. Ferreira A, Marguti I, Bechmann I, Jeney V, Chora A, Palha NR, Rebelo S, Henri A, Beuzard Y, Soares MP. 2011. Sickle hemoglobin confers tolerance to *Plasmodium* infection. Cell 145:398–409. https://doi.org/10.1016/j.cell.2011.03.049.
39. Spritz RA, DeRiel JK, Forget BG, Weissman SM. 1980. Complete nucleotide sequence of the human delta-globin gene. Cell 21:639–646. https://doi.org/10.1016/0092-8674(80)90427-4.
40. Hardison RC. 2012. Evolution of hemoglobin and its genes. Cold Spring Harb Perspect Med 2:a011627. https://doi.org/10.1101/cshperspect.a011627.
41. Kloos WE. 1980. Natural populations of the genus *Staphylococcus*. Annu Rev Microbiol 34:559–592. https://doi.org/10.1146/annurev.mi.34.100180.003015.
42. Wright JS, III, Traber KE, Corrigan R, Benson SA, Musser JM, Novick RP. 2005. The agr radiation: an early event in the evolution of staphylococci. J Bacteriol 187:5585–5594. https://doi.org/10.1128/JB.187.16.5585-5594.2005.
43. van Belkum A, Melles DC, Nouwen J, van Leeuwen WB, van Wamel W, Vos MC, Wertheim HFL, Verbrugh HA. 2009. Co-evolutionary aspects of human colonisation and infection by *Staphylococcus aureus*. Infect Genet Evol 9:32–47. https://doi.org/10.1016/j.meegid.2008.09.012.
44. Weatherall D, Akinyanju O, Fucharoen S, Olivieri N, Musgrove P. 2006. Inherited disorders of hemoglobin, p 663–680. *In* Jamison DT, Breman JG, Measham AR, Alleyne G, Claeson M, Evans DB (ed), Disease control priorities in developing countries, 2nd ed. Oxford University Press and The World Bank, Washington, DC.
45. Stamatoyannopoulos G. 1972. The molecular basis of hemoglobin disease. Annu Rev Genet 6:47–70. https://doi.org/10.1146/annurev.ge.06.120172.000403.
46. Thom CS, Dickson CF, Gell DA, Weiss MJ. 2013. Hemoglobin variants: biochemical properties and clinical correlates. Cold Spring Harb Perspect Med 3:a011858. https://doi.org/10.1101/cshperspect.a011858.
47. Perelman P, Johnson WE, Roos C, Seuánez HN, Horvath JE, Moreira MAM, Kessing B, Pontius J, Roelke M, Rumpler Y, Schneider MPC, Silva A, O'Brien SJ, Pecon-Slattery J. 2011. A molecular phylogeny of living primates. PLoS Genet 7:e1001342. https://doi.org/10.1371/journal.pgen.1001342.
48. Guindon S, Dufayard JF, Lefort V, Anisimova M, Hordijk W, Gascuel O. 2010. New algorithms and methods to estimate maximum-likelihood phylogenies: assessing the performance of PhyML 3.0. Syst Biol 59:307–321. https://doi.org/10.1093/sysbio/syq010.
49. Delport W, Poon AF, Frost SD, Kosakovsky Pond SL. 2010. Datamonkey 2010: a suite of phylogenetic analysis tools for evolutionary biology. Bioinformatics 26:2455–2457. https://doi.org/10.1093/bioinformatics/btq429.
50. Pond SL, Frost SD, Muse SV. 2005. HyPhy: hypothesis testing using phylogenies. Bioinformatics 21:676–679. https://doi.org/10.1093/bioinformatics/bti079.
51. Pettersen EF, Goddard TD, Huang CC, Couch GS, Greenblatt DM, Meng EC, Ferrin TE. 2004. UCSF Chimera–a visualization system for exploratory research and analysis. J Comput Chem 25:1605–1612. https://doi.org/10.1002/jcc.20084.
52. Villarreal DM, Phillips CL, Kelley AM, Villarreal S, Villaloboz A, Hernandez P, Olson JS, Henderson DP. 2008. Enhancement of recombinant hemoglobin production in *Escherichia coli* BL21(DE3) containing the *Plesiomonas shigelloides* heme transport system. Appl Environ Microbiol 74:5854–5856. https://doi.org/10.1128/AEM.01291-08.
53. Kreiswirth BN, Löfdahl S, Betley MJ, O'Reilly M, Schlievert PM, Bergdoll MS, Novick RP. 1983. The toxic shock syndrome exotoxin structural gene is not detectably transmitted by a prophage. Nature 305:709–712. https://doi.org/10.1038/305709a0.
54. Duthie ES, Lorenz LL. 1952. Staphylococcal coagulase: mode of action and antigenicity. J Gen Microbiol 6:95–107. https://doi.org/10.1099/00221287-6-1-2-95.
55. Bubeck Wardenburg J, Williams WA, Missiakas D. 2006. Host defenses against *Staphylococcus aureus* infection require recognition of bacterial lipoproteins. Proc Natl Acad Sci U S A 103:13831–13836. https://doi.org/10.1073/pnas.0603072103.